# Detection of southward intracontinental subduction of Tibetan lithosphere along the Bangong-Nujiang suture by P-to-S converted waves

Danian Shi* Institute of Mineral Resources, Chinese Academy of Geological Sciences, 26 Baiwanzhuang Road, Beijing 100037, China, and China University of Geosciences, Beijing 100083, China
Wenjin Zhao Chinese Academy of Geological Sciences, 26 Baiwanzhuang Road, Beijing 100037, China
Larry Brown Department of Geological Sciences, Cornell University, Ithaca, New York 14853, USA
Doug Nelson† Department of Earth Sciences, Syracuse University, Syracuse, New York 13244, USA
Xun Zhao Chinese Academy of Geological Sciences, 26 Baiwanzhuang Road, Beijing 100037, China
Rainer Kind GeoForschungsZentrum Potsdam (GFZ), Telegrafenberg, 14473 Potsdam, Germany
James Ni Department of Physics, New Mexico State University, Las Cruces, New Mexico 88003, USA
Jiayu Xiong Chinese Academy of Geological Sciences, 26 Baiwanzhuang Road, Beijing 100037, China
James Mechie GeoForschungsZentrum Potsdam (GFZ), Telegrafenberg, 14473 Potsdam, Germany
Jinru Guo Department of Geological Sciences, Cornell University, Ithaca, New York 14853, USA
Simon Klemperer Department of Geophysics, Stanford University, Stanford, California 94305, USA
Tom Hearn Department of Physics, New Mexico State University, Las Cruces, New Mexico 88003, USA

## ABSTRACT

**Teleseismic primary (P) to secondary (S) converted waves recorded on the INDEPTH III seismic array have been used to detect lithospheric-scale deformation structures of the central Tibetan Plateau from the central Lhasa terrane to the central Qiangtang terrane. A south-dipping crustal converter is seen from the upper crust near the 500-km-long metamorphic core complex exposures in the Qiangtang terrane to the lower crust near the Bangong-Nujiang suture. At deeper depths, a southeast-dipping mantle converter is seen extending from ~50 km north of the Bangong-Nujiang suture at the depth of the Moho, to a depth of ~180 km, ~100 km south of the Bangong-Nujiang suture. We found the observations to be most consistent with a model of lithospheric deformation involving (1) southward subduction of the Tibetan lithospheric mantle along the Bangong-Nujiang suture and (2) thickening of the central Tibetan crust through a thick-skinned, crustal accretionary thrust-wedge structure in response to the India's collision with Asia.**

**Keywords:** receiver function, lithospheric structure, continental collision, Tibetan Plateau.

## INTRODUCTION

Tibet is Earth's largest and highest plateau; its existence is a direct consequence of the India-Asia collision, ongoing since ca. 55 Ma. Knowledge of the structure and evolution of the plateau has advanced through a number of modern geophysical studies (see Molnar, 1988, for a review; Zhao et al., 1993; McNamara et al., 1994; Hirn et al., 1995; Wittlinger et al., 1996; Brown et al., 1996). However, how the plateau's crust was thickened and how its uniform altitude was attained remain unsolved problems in the mechanics of continental deformation. A recent model relates the uplift of the plateau to a plate-like behavior including sequential intracontinental subductions with slip partitioning (Tapponnier et al., 2001), in contrast to a distributed shortening of the entire lithosphere followed by convective thinning of the lithospheric root (England and Houseman, 1989). Previous works support a southward subduction of Eurasian mantle lithosphere beneath the northern margin of the plateau (Kosarev et al., 1999; Kind et al., 2002). However, direct seismic evidence for the postulated intracontinental subduction zones within the plateau, such as a southward subduction of the Tibetan lithospheric mantle along the Bangong-Nujiang suture, is still lacking.

During 1998–1999, project INDEPTH III deployed a dense passive-source seismic array across the Bangong-Nujiang suture from the central Lhasa terrane to the central Qiangtang terrane (Fig. 1). The array

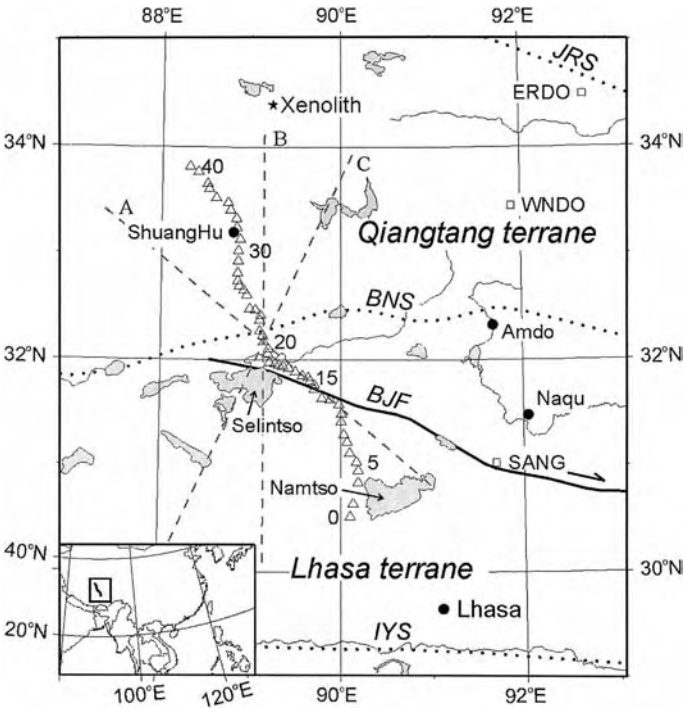


**Figure 1. Map of central Tibetan Plateau. Triangles indicate INDEPTH III seismological stations. Dashed gray lines centered at station 20 represent orientations of three cross sections in Figure 2. Dotted lines represent Indus-Yarlung-Tsangpo suture (IYS), Bangong-Nujiang suture (BNS), and Jinsha River suture (JRS). Thick solid line marks Bengco-Jiali right-lateral strike-slip fault (BJF). Thin solid lines are rivers, and gray-shaded areas are lakes. Rectangles mark 1991–1992 PASSCAL stations (McNamara et al., 1994). Star denotes xenolith location described by Hacker et al. (2000).**

*E-mail: shidanian@cags.cn.net.
†Deceased 18 August 2002.

crosses a region of central Tibet where upper-mantle properties change dramatically from south to north (see Molnar, 1988, for a review; Owens and Zandt, 1997; Huang et al., 2000). This region was previously suggested to be where the front of Indian lithosphere has advanced (Ni and Barazangi, 1983; Owens and Zandt, 1997; Kosarev et al., 1999). The results from this array enable us to image the deformation structures in this region in greater detail and to test the validity of the geodynamic models.

## DATA AND ANALYSIS

The data used in this study are from the INDEPTH III main seismic array, which consisted of 54 stations and extended north-northwestward for ~400 km across the Bangong-Nujiang suture (Fig. 1). This quasi-linear array was operated to record earthquake data continuously for one year.

We used the receiver function (RF) technique (Langston, 1977; Kosarev et al., 1999; Kind et al., 2002) to construct crust-mantle cross sections of the central Tibetan Plateau. This method has been used to image the mantle discontinuities and the first-order features of the entire plateau (Kosarev et al., 1999; Kind et al., 2002). To reveal the deformation structures over the entire thickness of the lithosphere, we used several methods to construct cross sections with higher resolution. First, spatial (especially horizontal) averaging over a long distance (which is a common way to achieve a good-looking image) has been avoided because it will smear the dipping structures on the cross sections. Second, a high-pass Butterworth filter (0.02 Hz) was applied to the original seismic data in the RF calculation to suppress extremely low frequency noises. Unlike high-frequency noise, extremely low frequency noise cannot be suppressed readily in the stacking process of the construction of a RF cross section. The filtering in this case has negligible effects on the signal but makes many more data available. Retrieving sufficient data, in our experience, is essentially necessary to detect the weak signal from the mantle and to recover the mantle structures. Third, the cross section (a vertical plane to project all the data; migrated RFs are stacked along the normal direction of that plane) has been rotated along different azimuths to detect the strike of dipping structures, because in principle a dipping structure can only be optimally imaged on the cross section that is perpendicular to the structure's strike (see Data Repository[1]). In order to retain the signal coherence for two-dimensional dipping structure, only earthquakes from the east were used. This implies that the cross section is representative of structures below and slightly east of the array (possibly not below the cross section) (Fig. DR3; see footnote 1). The cross sections that best demonstrate the lithospheric deformation structures of central Tibet are presented in Figure 2.

## RESULTS

The Moho delineated by the maximum amplitude is seen differently beneath the northern Lhasa terrane and the southern Qiangtang terrane (Figs. 2 and DR5 [see footnote 1]). The Moho beneath the northern Lhasa terrane is shown to be relatively weak and irregularly and unevenly distributed around an average depth of ~65 ± 3 km below sea level. In contrast, the Moho beneath the southern Qiangtang terrane is shown to be relatively strong, regular, and smooth, and dipping slightly to the south. A trough in the Moho between them is seen ~40 km north of the surface trace of the Bangong-Nujiang suture. The irregularity and unevenness of the Moho beneath the northern Lhasa terrane, in principle, can be ascribed to a variation in crustal velocity, e.g., a variation in the crustal $V_p/V_s$ ratio (Kind et al., 2002), a variation in Moho depth, or both. Heterogeneity in the crust, however, cannot account for our results completely. The image in Figure 2C as well as the scattered energy in Figure 2A tend to suggest that a small fault offset in the Moho probably exists under the Bengco-Jiali fault. The Moho appears to be ~5 ± 3 km deeper on the north side of that fault.

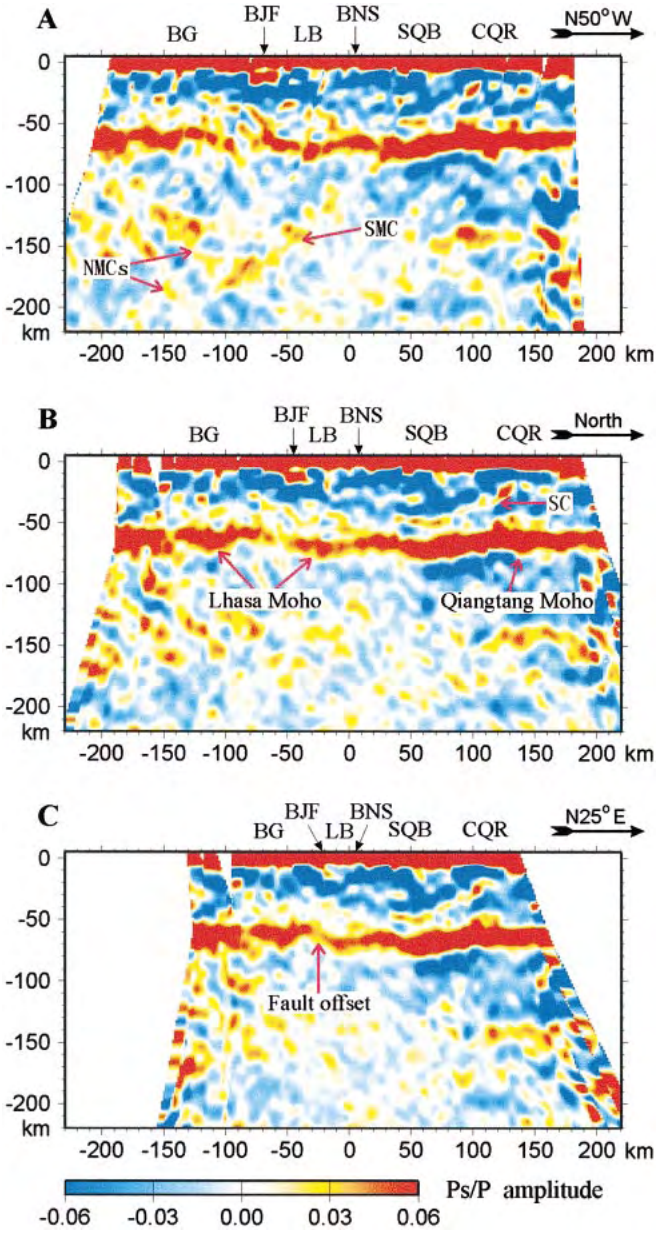


**Figure 2. Receiver function (RF) images of central Tibetan Plateau constructed along three different azimuths, showing three different structures. Origin of each cross section is set horizontally to station 20 (89.14227°E, 32.16955°N) and vertically to sea level (see Fig. 1). In cross section, dipping structure is best shown most nearly perpendicular to its strike. A: Southeast-dipping mantle converter (SMC) and some approximately north-dipping mantle converters (NMCs). BNS—Bangong-Nujiang suture; BG—Bango granite; BJF——Bengco-Jiali fault; LB—Lumpola basin; SQB—southern Qiangtang basin; CQR—central Qiangtang rise. B: South-dipping intracrustal converter (SC). C: Small fault offset of ~5 ± 3 km in Moho across BJF. In construction of these images, RFs were migrated with average crustal velocities of $V_p$ = 6.2 and $V_s$ = 3.543 km/s. Previous seismic experiments have shown that average crustal $V_p$ in Tibet ranges from 6.0 to 6.4 km/s (Zhao et al., 2001); therefore, variation of ±0.2 km/s in crustal $V_p$ may exist. Total of 2062 RFs from 91 earthquakes was used.**

[1]GSA Data Repository item 2004034, further descriptions of data and analysis, is available online at www.geosociety.org/pubs/ft2004.htm, or on request from editing@geosociety.org or Documents Secretary, GSA, P.O. Box 9140, Boulder, CO 80301-9140, USA.

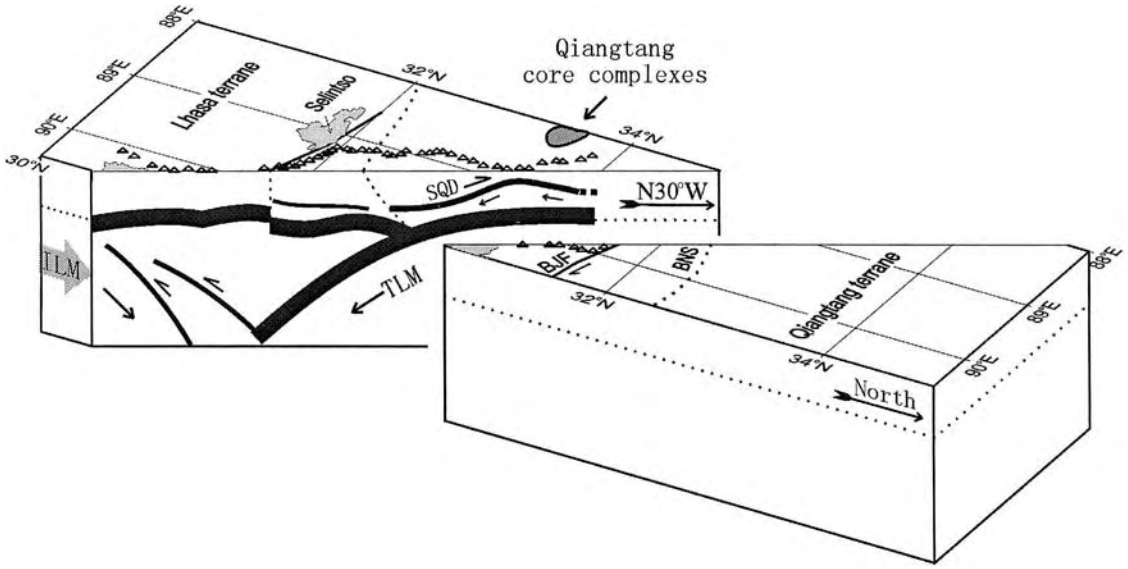


**Figure 3. Schematic lithospheric section of central Tibetan Plateau with deformation structures inferred from receiver function imaging (Fig. DR6; see footnote 1). SQD—southern Qiangtang detachment; BJF—Bengco-Jiali fault; BNS—Bangong-Nujiang suture; ILM—Indian lithospheric mantle; TLM—Tibetan lithospheric mantle.**

On the south-north cross section (Fig. 2B), a south-dipping crustal converter (P-to-S conversion boundary) is imaged beneath the southern Qiangtang terrane from ~15 ± 3 km to ~45 ± 3 km below sea level. It forms a dome beneath the central Qiangtang rise, before it becomes unconstrained farther north.

At greater depths, a weak southeast-dipping mantle converter (SMC) is shown on the image in Figure 2A, which extends from the southern end of the Qiangtang Moho to a depth of ~180 km, ~100 km south of the Bangong-Nujiang suture. The image in Figure 2A also shows some approximately north-dipping mantle converters in contrast to the south-dipping mantle converter.

## DISCUSSION AND CONCLUSIONS

The Moho structure revealed by our results received support from the INDEPTH III P-wave wide-angle profiling, which also showed two similar changes in Moho depths under the Bengco-Jiali fault and ~40 km north of the Bangong-Nujiang suture (Zhao et al., 2001). The similarities were shown despite the fact that the techniques are methodically different—our study is relatively sensitive to the S-wave velocity structure, whereas the INDEPTH wide-angle profiling is related to the P-wave velocity structure only. The Bengco-Jiali fault is a seismically active Quaternary fault (Armijo et al., 1989). The small fault offset in the Moho across the Bengco-Jiali fault is most clearly imaged on the cross section perpendicular to its surface trace (Fig. 2C). Therefore, it probably resulted from the right-lateral strike-slip shear along the fault, perhaps owing to a lateral variation in the Moho depth or a small vertical slip component along the fault. This observation supports the hypothesis that the Bengco-Jiali fault is a major lithospheric boundary, as suggested by Armijo et al. (1989). The Bangong-Nujiang suture is thought to have formed during the Late Jurassic–Early Cretaceous convergence between the Lhasa and Qiangtang terranes (Girardeau et al., 1984; Dewey et al., 1988). The trough in the Moho ~40 km north of the surface trace of the Bangong-Nujiang suture is most likely associated with that suture, according to the conversion characteristics of the Moho or the crust and upper-mantle structures. This interpretation is more or less consistent with the geological observation that ophiolitic rocks were emplaced southward over the northern Lhasa terrane (Girardeau et al., 1984). Our results show no evidence of a northward step-up in the Moho of ~20 km across the Bangong-Nujiang suture, as inferred from seismic fan profiling (Hirn et al., 1984). The reflection from the depth of ~50 km on the north of the Bangong-Nujiang suture in the previous fan profile (Hirn et al., 1984) is, according to our results, more likely from the intracrustal structure than from the Moho.

The southeast-dipping mantle converter, although weak owing to the small velocity contrast across it, is coherent and can be traced readily from the Qiangtang Moho. This finding might be suggestive of a southeastward subduction of the Tibetan lithospheric mantle along the Bangong-Nujiang suture. Using the INDEPTH data, Tilmann et al. (2003) constructed a tomographic image for the same region, which exhibits two subvertical-dipping high-velocity bodies in the upper mantle. The tops of the two bodies coincide well with the southeast-dipping and the north-dipping mantle converters in our results. The surface trace of the Bangong-Nujiang suture shows a northeast trend in this area (Fig. 1). Therefore, we suggest that the northeast strike (or southeast dip) of the Tibetan mantle slab imaged here might be a manifestation of its crooked geometry in the mantle, and comparable to that observed at the surface for the Bangong-Nujiang suture.

The north-dipping mantle converters are seen as a compound of energy and appear to be more complicated than would be expected from a single boundary, as suggested by an earlier RF study on a profile ~100 km to the east (Kosarev et al., 1999). An alternative interpretation is that these north-dipping converters reflect the stacking structures resulting from the collision between the Indian lithospheric mantle (being subducted from the south) and the Tibetan lithospheric mantle (being subducted from the north) (Fig. 3). The Indian lithospheric mantle has most likely been subducted along the southern margin of these complicated structures (also see Kosarev et al., 1999). The top of the subducted Indian lithospheric mantle (as well as some north-dipping intracrustal structures) cannot be well constrained, probably owing to negligible P-to-S-wave conversion amplitudes for near-normal incidence (Langston, 1977) because the seismic waves used in this study come mostly from the southeast or from the Pacific region. This interpretation of the interaction of the two colliding lithospheres seems more compatible with interpretations previously advocated for many geophysical observations (see Molnar, 1988; Owens and Zandt, 1997; Kind et al., 2002), e.g., the additional force needed to bend down the Indian plate to support the excess height of the Himalayan Range (Molnar, 1988).

The south-dipping crustal converter is the most clearly imaged intracrustal interface, extending from the upper crust to the lower crust

beneath the southern Qiangtang terrane. The central Qiangtang rise is characterized by a 500-km-long band of blueschist-bearing metamorphic core complexes. Geological observations suggest that the rise consists of accretionary mélange underplated to the lower crust of the Qiangtang terrane during the early Mesozoic southward subduction of oceanic lithosphere along the Jinsha River suture and subsequently exhumed to the surface by detachment faulting (Kapp et al., 2000). This idea has received support from the petrologic observation that suggests that the lower crust of the Qiangtang terrane consists of anhydrous metasedimentary rocks (Hacker et al., 2000). The south-dipping crustal converter in our image may represent that detachment fault beneath the southern Qiangtang terrane. The south-dipping crustal converter discovered in this study would have major implications for paleotectonic reconstruction and study on the present-day composition and structure of the central Tibetan crust.

A further striking feature of the south-dipping crustal converter is that it becomes flatter as it dips into the lower crust (Fig. 2). The most plausible interpretation is that it resulted from lower crustal flow, i.e., an originally moderately dipping structure (detachment) has been ''stretched out'' by flow, as proposed by Clark and Royden (2000).

In summary, our results suggest an accretionary thrust-wedge type structure in central Tibet; this structure may have formed during the Mesozoic and then may have been reactivated as India penetrated Asia during the Cenozoic. According to our results, the deformation and crustal thickening of central Tibet may have occurred through thrust faulting of an accretionary wedge, and the Bengco-Jiali fault seems to be a consequence of the oblique confrontation of the two subducted lithospheric mantles along the zone of lithospheric weakness between them. The latter can also account for the large amount of transcurrent shear along the Bengco-Jiali fault and the sharp change in seismic anisotropy across that fault observed by Huang et al. (2000). The south-dipping Tibetan mantle slab discovered in this study and its obstruction may also help to explain why the Indian lithosphere cannot subduct farther north, since the crust and upper mantle of northern Tibet is weak.

Our results seem to support the three-phase Tibet-rise model (Tapponnier et al., 2001), in that an earlier rise phase of the plateau occurred through southward subduction of the Tibetan mantle slab along the Bangong-Nujiang suture, and crustal thickening occurred through thrust emplacement of a crustal wedge after the indention of Asia by India.

The great flatness of the broad plateau may be partly ascribed to adjustments along huge, mountain-parallel crustal faulting systems, including normal faulting along the South Tibetan detachment system (Burchfiel et al., 1992), thrusting along many thrust faults in southern Tibet, as shown on the INDEPTH reflection profile (Brown et al., 1996), and thrusting along the southern Qiangtang detachment, as imaged here.

**ACKNOWLEDGMENTS**

We thank Yu Qinfan for providing constructive suggestions during preparation of the manuscript. Project INDEPTH III is supported by the Ministry of Land and Resources of the People's Republic of China, the U.S. National Science Foundation Continental Dynamics Program, and the Deutsche Forschungsgemeinschaft and GeoForschungsZentrum Potsdam (GFZ), Germany. Instruments were provided by IRIS-PASSCAL and the GFZ Potsdam geophysical instrument pool. Figure 1 was prepared by using the GMT software package. We thank two anonymous reviewers for helpful feedback that greatly improved the manuscript.

**REFERENCES CITED**

Armijo, R., Tapponnier, P., and Han, T., 1989, Late Cenozoic right-lateral strike-slip faulting in southern Tibet: Journal of Geophysical Research, v. 94, p. 2787–2838.

Brown, L.D., Zhao, W., Nelson, K.D., Hauck, M., Alsdorf, D., Ross, A., Cogan, M., Clark, M., Liu, X., and Che, J., 1996, Bright spots, structure, and magmatism in southern Tibet from INDEPTH seismic reflection profiling: Science, v. 274, p. 1688–1690.

Burchfiel, B.C., Chen, Z., Hodges, K.V., Liu, Y., Royden, L.H., Deng, C., and Xu, J., 1992, The South Tibetan detachment system, Himalayan orogeny: Extension contemporaneous with and parallel to shortening in a collisional mountain belt: Geological Society of America Special Paper v. 269, p. 1–41.

Clark, M.K., and Royden, L.H., 2000, Topographic ooze: Building the eastern margin of Tibet by lower crustal flow: Geology, v. 28, p. 703–706.

Dewey, J.F., Shackleton, R.M., Chang, C., and Sun, Y., 1988, The tectonic evolution of the Tibetan Plateau: Royal Society of London Philosophical Transactions, ser. A, v. 327, p. 379–413.

England, P.C., and Houseman, G.A., 1989, Extension during continental convergence, with application to the Tibetan Plateau: Journal of Geophysical Research, v. 94, p. 17,561–17,579.

Girardeau, J., Marcoux, J., Allegre, C.J., Bassoullet, J.P., Tang, Y., Xiao, X., Zao, Y., and Wang, X., 1984, Tectonic environment and geodynamic significance of the Neo-Cimmerian Donqiao ophiolite, Bangong-Nujiang suture zone, Tibet: Nature, v. 307, p. 27–31.

Hacker, B.R., Gnos, E., Ratschbacher, L., Grove, M., McWillams, M., Sobolev, S.V., Jiang, W., and Wu, Z., 2000, Hot and dry deep crustal xenoliths from Tibet: Science, v. 287, p. 2463–2466.

Hirn, A., Nercessian, A., Sapin, M., Jobert, G., Xu, Z., Gao, E., Lu, D., and Teng, J., 1984, Lhasa block and bordering sutures—A continuation of a 500-km Moho traverse through Tibet: Nature, v. 307, p. 25–27.

Hirn, A., Jiang, M., Sapin, M., Diaz, J., Nercessian, A., Lu, Q., Lepine, J.C., Shi, D., Sachpazi, M., Pandey, M.R., Ma, K., and Gallart, J., 1995, Seismic anisotropy as an indicator of mantle flow beneath the Himalayas and Tibet: Nature, v. 375, p. 571–574.

Huang, W.C., Ni, J., Tilmann, F., Nelson, D., Guo, J., Zhao, W., Mechie, J., Kind, R., Saul, J., Rapine, R., and Hearn, T., 2000, Seismic polarization anisotropy beneath the central Tibetan Plateau: Journal of Geophysical Research, v. 105, p. 27,979–27,989.

Kapp, P., Yin, A., Manning, C.E., Murphy, M., Harrison, T.M., Spurlin, M., Ding, L., Deng, X., and Wu, C., 2000, Blueschist-bearing metamorphic core complexes in the Qiangtang block reveal deep crustal structure of northern Tibet: Geology, v. 28, p. 19–22.

Kind, R., Yuan, X., Saul, J., Nelson, D., Sobolev, S.V., Mechie, J., Zhao, W., Kosarev, G., Ni, J., Achauer, U., and Jiang, M., 2002, Seismic images of crust and upper mantle beneath Tibet: Evidence for Eurasian plate subduction: Science, v. 298, p. 1219–1221.

Kosarev, G., Kind, R., Sobolev, S.V., Yuan, X., Hanka, W., and Oreshin, S., 1999, Seismic evidence for a detached Indian lithospheric mantle beneath Tibet: Science, v. 283, p. 1306–1309.

Langston, C.A., 1977, The effect of planar dipping structure on source and receiver responses for constant ray parameter: Seismological Society of America Bulletin, v. 67, p. 1029–1050.

McNamara, D.E., Owens, T.J., Silver, P.G., and Wu, F.T., 1994, Shear wave anisotropy beneath the Tibetan Plateau: Journal of Geophysical Research, v. 99, p. 13,655–13,665.

Molnar, P., 1988, A review of geophysical constraints on the deep structure of the Tibetan Plateau, the Himalaya and the Karakoram, and their tectonic implications: Royal Society of London Philosophical Transactions, ser. A, v. 326, p. 33–88.

Ni, J., and Barazangi, M., 1983, High-frequency seismic wave propagation beneath the Indian Shield, Himalayan arc, Tibetan Plateau and surrounding regions: High uppermost mantle velocities and efficient Sn propagation beneath Tibet: Royal Astronomical Society Geophysical Journal, v. 72, p. 665–689.

Owens, T.J., and Zandt, G., 1997, Implications of crustal property variations for models of Tibetan Plateau evolution: Nature, v. 387, p. 37–43.

Tapponnier, P., Xu, Z., Roger, F., Meyer, B., Arnaud, N., Wittlinger, G., and Yang, J., 2001, Oblique stepwise rise and growth of the Tibet Plateau: Science, v. 294, p. 1671–1677.

Tilmann, F., Ni, J., and INDEPTH III Seismic Team, 2003, Seismic imaging of the downwelling Indian lithosphere beneath central Tibet: Science, v. 300, p. 1424–1427.

Wittlinger, G., Masson, F., Poupinet, G., Tapponnier, P., Jiang, M., Herquel, G., Guibert, J., Achauer, U., Xue, G., and Shi, D., 1996, Seismic tomography of northern Tibet and Kunlun: Evidence for crustal blocks and mantle velocity contrasts: Earth and Planetary Science Letters, v. 139, p. 263–279.

Zhao, W., Nelson, K.D., and Project INDEPTH Team, 1993, Deep seismic reflection evidence for continental underthrusting beneath southern Tibet: Nature, v. 366, p. 557–559.

Zhao, W., Mechie, J., Brown, L.D., Guo, J., Haines, S., Hearn, T., Klemperer, S.L., Ma, Y., Meissner, R., Nelson, K.D., Ni, J.F., Pananont, P., Rapine, R., Ross, A., and Saul, J., 2001, Crustal structure of central Tibet as derived from project INDEPTH wide-angle seismic data: Geophysical Journal International, v. 145, p. 486–498.

Manuscript received 14 May 2003
Revised manuscript received 11 November 2003
Manuscript accepted 14 November 2003

Printed in USA

DR2004034

# Data Repository Items

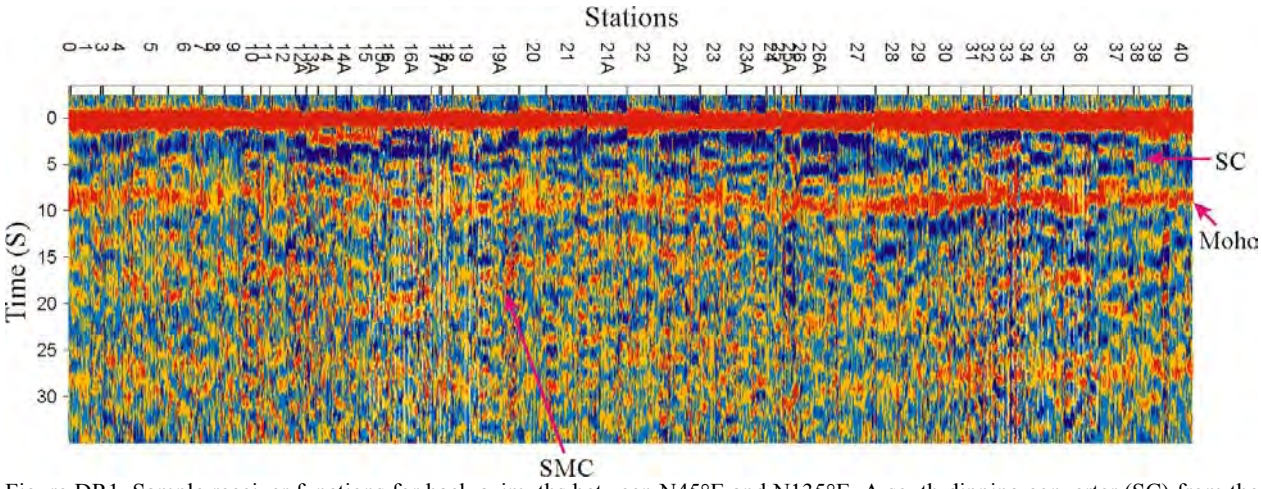


Figure DR1. Sample receiver functions for back-azimuths between N45°E and N135°E. A south-dipping converter (SC) from the upper to the lower crust of the Qiangtang terrane is shown clearly. A south-dipping mantle converter (SMC) is discernible as well. In the receiver function calculation, the Gaussian filter factor $\alpha$ and the water level factor $c$ are set to 1.5 and 0.05, respectively.

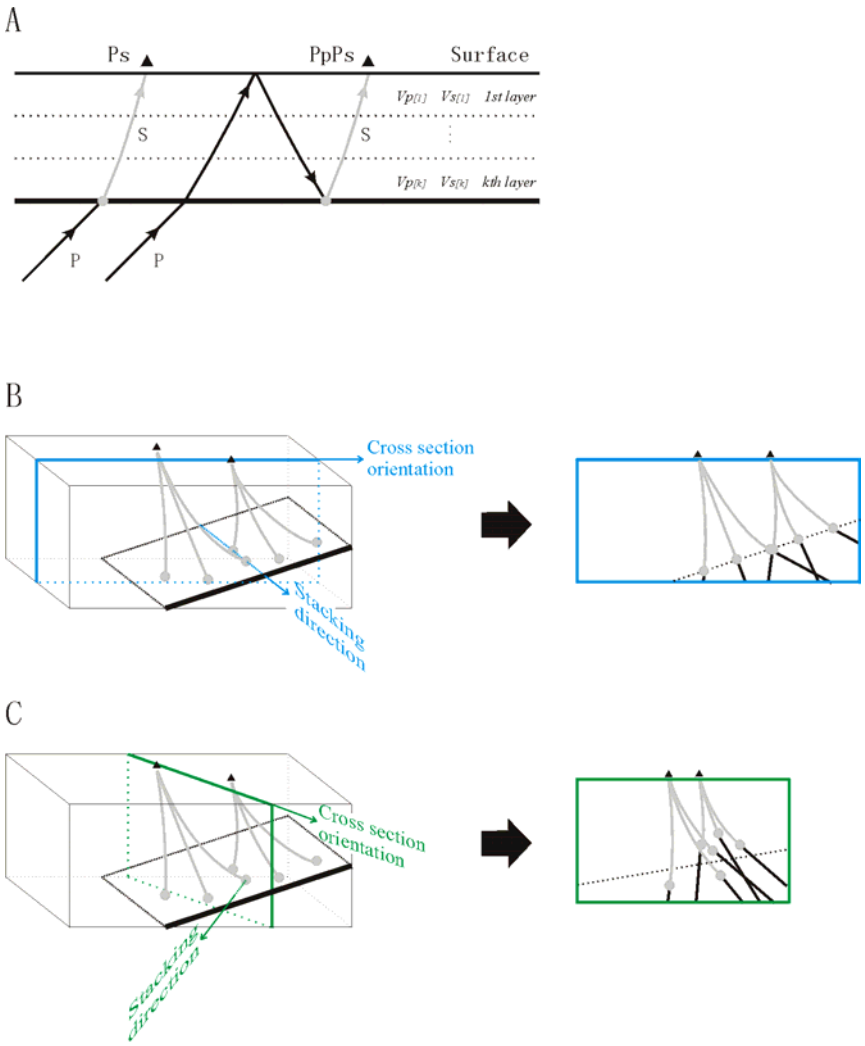


Figure DR2. Diagrams for the construction of receiver function cross sections in this study. A: Ray paths of the directly converted Ps wave and the multiple converted PpPs phase in a layered medium, on the basis of which receiver functions are migrated into spatial image. B: Dipping structure imaged on the cross section (a projective vertical plane) perpendicular to the strike of the dipping structure. C: Dipping structure imaged on the cross section oblique to the strike of the structure. In the cross section construction, receiver functions are stacked (averaged) along the normal direction of the vertical plane. Therefore, dipping structure will be imaged more coherently on the former cross section than on the later one. Although sometimes the layered medium migration method may yield somewhat dip-shift for dipping structure on the image (comparable to of that in seismic reflection profiling), this method is still preferable because it recovers correctly (or frankly) the geometry of (sub-) horizontal structures. Usually, the impairment on the signal coherence for dipping structure due to the migration error can be reduced by using only earthquakes whose backazimuths within a special range in the stacking (ref. Langston 1977; Nabelek, et al., 1993, EOS Trans. AGU, v. 74, p. 431).

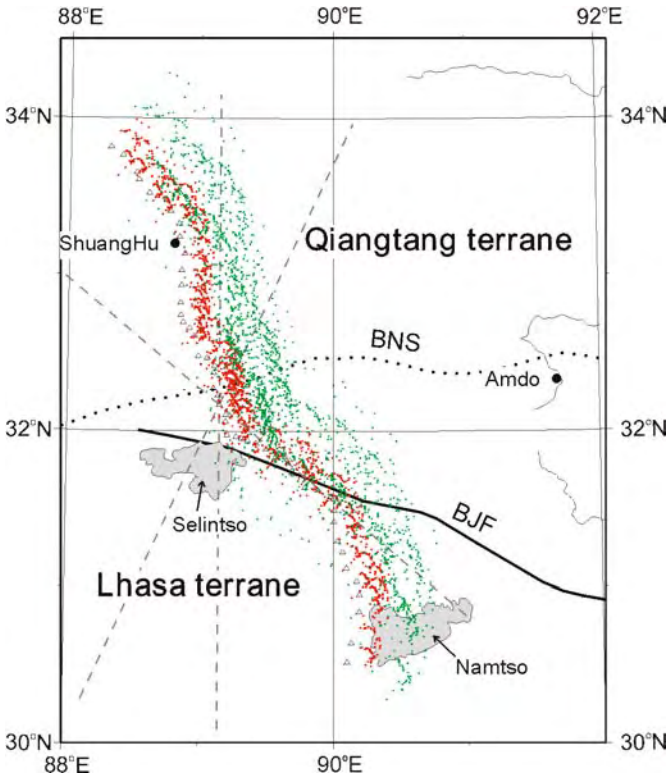


Figure DR3. Location of piercing points of P-to-S converted waves at 65- (red) and 150- km (green) depths below sea level (migrated with layered velocity model), indicating that the receiver functions sample (or represent) subsurface structures below and just east of the quasi-linear array. Triangles indicate INDEPTH III seismological stations. Dashed gray lines represent the orientations of the three cross sections. Dotted line represents Bangong-Nujiang suture (BNS). Thick solid line marks Bengco-Jiali right-lateral strike slip fault (BJF). Thin solid lines are rivers, and gray- shaded areas are lakes.

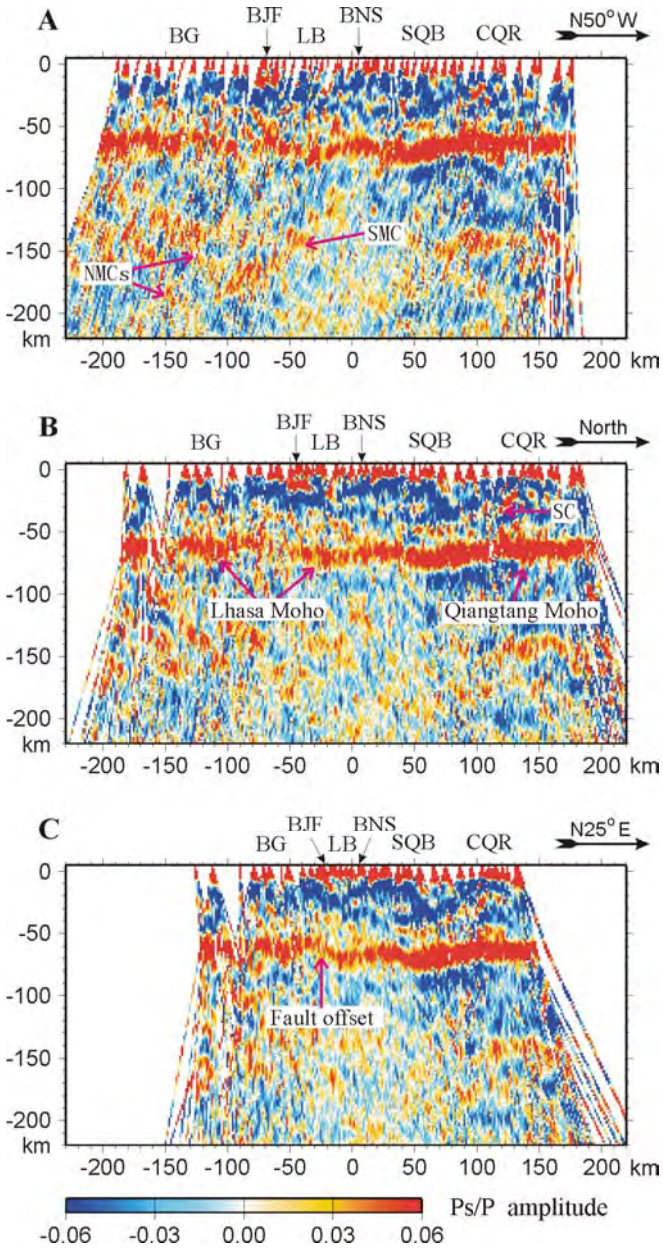


Figure DR4. Cross sections similar to of those shown in Fig. 2 but constructed with smaller stacking bin size. BJF—Bengco-Jiali fault; BNS—Bangong-Nujiang suture; BG—Bango granite; LB—Lumpola basin; SQB—southern Qiangtang basin; CQR—central Qiangtang rise.

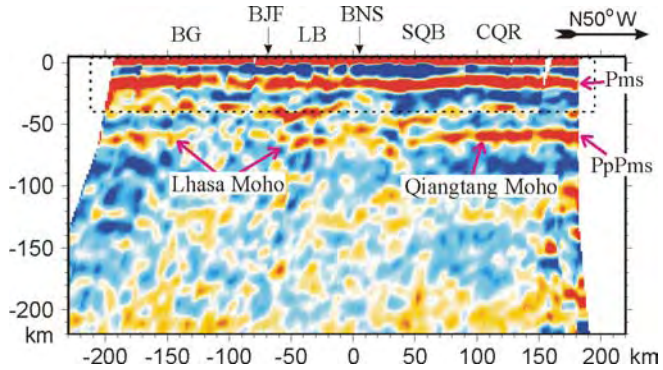


Figure DR5. Moho imaged with multiple conversion PpPms phase. Different conversion characteristics of Lhasa Moho and Qiangtang Moho are shown as distinctly as in image using direct-conversion Pms phase (Fig. 2). All the data in this cross section are migrated for the multiple converted PpPs phases. Therefore, the multiple converted PpPms phase should be correctly migrated in this image, but the directly converted phases (including Pms) should be mis-positioned (mostly enclosed in the dashed rectangle). BJF—Bengco-Jiali fault; BNS—Bangong-Nujiang suture; BG—Bango granite; LB—Lumpola basin; SQB—southern Qiangtang basin; CQR—central Qiangtang rise.

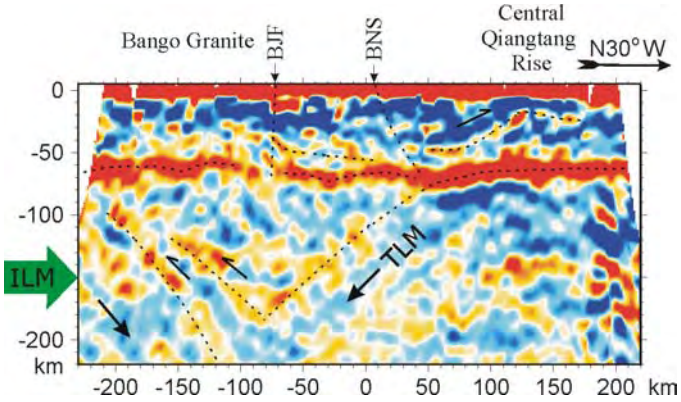


Figure DR6. Cross section constructed along the array and the correspondent deformation structures shown in Fig.3.